

# Narrowband high-fidelity all-fibre source of heralded single photons at 1570 nm

A.R. McMillan<sup>1</sup>, J. Fulconis<sup>2</sup>, M. Halder<sup>2</sup>, C. Xiong<sup>1</sup>, J.G. Rarity<sup>2</sup> and W.J. Wadsworth<sup>1</sup>

<sup>1</sup>Centre for Photonics and Photonic Materials, Department of Physics,  
University of Bath, Claverton Down, Bath, BA2 7AY, UK

<sup>2</sup>Centre for Communications Research, Department of Electrical and Electronic Engineering, University of Bristol,  
Merchant Venturers Building, Woodland Road, Bristol, BS8 1UB, UK  
[a.r.mcmillan@bath.ac.uk](mailto:a.r.mcmillan@bath.ac.uk)

**Abstract:** An all-fibre heralded single photon source operating at 1570 nm has been demonstrated. The device generates correlated photon pairs, widely spaced in frequency, through four-wave mixing in a photonic crystal fibre. Separation of the pair photons and narrowband filtering is all achieved in fibre. The output heralded single photon rate was  $9.2 \times 10^4$  per second, with a counts-to-accidentals ratio of 10.4 and a heralding fidelity of 52%. Furthermore, narrowband filtering ensured that the output single photon state was near time-bandwidth limited with a coherence length of 4 ps. Such a source is well suited to quantum information processing applications.

©2009 Optical Society of America

**OCIS codes:** (270.5585) Quantum optics. Quantum information and processing; (060.5565) Fibre optics. Quantum comm.

---

## References and links

1. S. A. Castelletto and R. E. Scholten, "Heralded single photon sources: a route towards quantum communications technology and photon standards," *Eur. Phys. J. Appl. Phys.* **41**, 181-194 (2008).
2. A. K. Ekert, J. G. Rarity, P. R. Tapster, and G. M. Palma, "Practical quantum cryptography based on two-photon interferometry," *Phys. Rev. Lett.* **69**, 1293-1295 (1992).
3. N. Gisin, G. Ribordy, W. Tittel, and H. Zbinden, "Quantum cryptography," *Rev. Mod. Phys.* **74**, 145-195 (2002).
4. T. Jennewein, C. Simon, G. Weihs, H. Weinfurter, and A. Zeilinger, "Quantum cryptography with entangled photons," *Phys. Rev. Lett.* **84**, 4729-4732 (2000).
5. S. Gasparoni, J. W. Pan, P. Walther, T. Rudolph, and A. Zeilinger, "Realization of a photonic controlled-NOT gate sufficient for quantum computation," *Phys. Rev. Lett.* **93**, 020504 (2004).
6. J. Chen, J. B. Altepeter, M. Medic, K. F. Lee, B. Gokden, R. H. Hadfield, S. W. Nam, and P. Kumar, "Demonstration of a quantum controlled-NOT gate in the telecommunications band," *Phys. Rev. Lett.* **100**, 133603 (2008).
7. C. H. Bennett, G. Brassard, C. Crepéau, R. Jozsa, A. Peres, and W. K. Wootters, "Teleporting an unknown quantum state via dual classical and Einstein-Podolsky-Rosen channels," *Phys. Rev. Lett.* **70**, 1895-1899 (1993).
8. D. Bouwmeester, J. W. Pan, K. Mattle, M. Eibl, H. Weinfurter, and A. Zeilinger, "Experimental quantum teleportation," *Nature* **390**, 575-579 (1997).
9. K. Mattle, H. Weinfurter, P. G. Kwait, and A. Zeilinger, "Dense coding in experimental quantum communication," *Phys. Rev. Lett.* **76**, 4656-4959 (1996).
10. H. J. Briegel, W. Dür, J. I. Cirac, and P. Zoller, "Quantum repeaters: the role of imperfect local operations in quantum communications," *Phys. Rev. Lett.* **81**, 5932-5935 (1998).
11. J. L. O'Brien, "Optical quantum computing," *Science* **318**, 1567-1570 (2007).
12. E. Knill, R. Laflamme, and G. J. Milburn, "A scheme for efficient quantum computation with linear optics," *Nature* **409**, 46-52 (2001).
13. P. G. Kwait, K. Mattle, H. Weinfurter, A. Zeilinger, A. V. Sergienko, and Y. H. Shih, "New high-intensity source of polarization-entangled photon pairs," *Phys. Rev. Lett.* **75**, 4337-4342 (1995).
14. P. J. Mosley, J. S. Lundeen, B. J. Smith, P. Wasylczyk, A. B. U'Ren, C. Silberhorn, and I. A. Walmsley, "Heralded generation of ultrafast single photons in pure quantum states," *Phys. Rev. Lett.* **100**, 133601 (2008).
15. P. Michler, A. Kiraz, C. Becher, W. V. Schoenfeld, P. M. Petroff, L. Zhang, E. Hu, and A. Imamoglu, "A quantum dot single-photon turnstile device," *Science* **290**, 2282-2285 (2000).

16. S. Tanzilli, H. De Riedmatten, W. Tittel, H. Zbinden, P. Baldi, M. De Micheli, D. B. Ostrowsky, and N. Gisin, "Highly efficient photon-pair source using periodically poled lithium niobate waveguide," *Elec. Lett.* **37**, 26-28 (2001).
17. A. B. U'Ren, C. Silberhorn, K. Banaszek, and I. A. Walmsley, "Efficient conditional preparation of high-fidelity single photon states for fiber-optic quantum networks," *Phys. Rev. Lett.* **93**, 093601 (2004).
18. O. Alibart, D.B. Ostrowsky, P. Baldi, and S. Tanzilli, "High-performance guided-wave asynchronous heralded single-photon source," *Opt. Lett.* **30**, 1539-1541 (2005).
19. J. C. Knight, T. A. Birks, P. St. J. Russell, D. M. Atkin, "All-silica single-mode optical fiber with photonic crystal cladding," *Opt. Lett.* **21**, 1547-1549 (1996).
20. J. G. Rarity, J. Fulconis, J. Duligall, W. J. Wadsworth, and P. St. J. Russell, "Photonic crystal fiber source of correlated photon pairs," *Opt. Express* **13**, 534-544 (2005).
21. J. Fulconis, O. Alibart, W. J. Wadsworth, P. St. J. Russell, and J. G. Rarity, "High brightness single mode source of correlated photon pairs using a photonic crystal fiber," *Opt. Express* **13**, 7572-7582 (2005).
22. E. A. Goldschmidt, M.D. Eisaman, J. Fan, S. V. Polyakov, and A. Migdall, "Spectrally bright and broad fiber-based heralded single-photon source," *Phys. Rev. A* **78**, 013844 (2008).
23. J. D. Harvey, R. Leonhardt, S. Coen, G. K. L. Wong, J. C. Knight, W. J. Wadsworth, and P. St. J. Russell, "Scalar modulation instability in the normal dispersion regime by use of a photonic crystal fiber," *Opt. Lett.* **28**, 2225-2227 (2003).
24. W. J. Wadsworth, N. Joly, J. C. Knight, T. A. Birks, F. Biancalana, and P. St. J. Russell, "Supercontinuum and four-wave mixing with Q-switched pulses in endlessly single-mode photonic crystal fibres," *Opt. Express* **12**, 299-309 (2004).
25. J. Fulconis, O. Alibart, W.J. Wadsworth, and J. G. Rarity, "Quantum interference with photon pairs using two micro-structured fibres," *New J. Phys.* **9**, 276 (2007).
26. A. S. Clark, J. Fulconis, J. G. Rarity, W. J. Wadsworth, and J. L. O'Brien, "An all optical fibre quantum controlled-NOT gate," arXiv:quant-ph/0802.1676 (2008).
27. T. A. Birks, J. C. Knight, and P. St. J. Russell, "Endlessly single-mode photonic crystal fibre," *Opt. Lett.* **22**, 961-963 (1997).
28. M. Halder, A. Beveratos, R. Thew, C. Jorel, H. Zbinden, and N. Gisin, "High coherence photon pair source for quantum communication," *New J. Phys.* **10**, 023027 (2008).
29. S. Fasel, O. Alibart, S. Tanzilli, P. Baldi, A. Beveratos, N. Gisin, and H. Zbinden, "High-quality asynchronous heralded single-photon source at telecom wavelength," *New J. Phys* **6**, 163 (2004).
30. C. Xiong and W. J. Wadsworth, "Polarized supercontinuum in birefringent photonic crystal fibre pumped at 1064 nm and application to tuneable visible/UV generation," *Opt. Express* **16**, 2438-2445 (2008).

## 1. Introduction

Heralded single photon sources based on the generation of correlated photon pairs have been a subject of great interest and ongoing development due to their applications in quantum communications and particularly in quantum cryptography [1-4]. By taking advantage of the interference effect between photons from two such independent single photon sources it is possible to demonstrate other applications such as linear optical quantum logic gates [5,6], teleportation [7,8], dense coding [9], and quantum repeaters [10], which have uses both in the field of communications and quantum computing [11,12].

Historically the generation of heralded single photons has been most commonly achieved by using parametric down-conversion (PDC) through the  $\chi^{(2)}$  nonlinearity in bulk crystals [13,14]. Other types of sources including quantum dots [15], atoms or ions in cavities, and periodically-poled waveguides [16-18] have also been demonstrated. Unfortunately many of these photon sources are limited by poor coupling efficiencies to single-mode optical fibre. This is particularly relevant for communications applications where compatibility with existing telecommunications networks is highly desirable. The best heralding fidelities for waveguide devices operating near 1550 nm are currently around 40 % [18].

Fibre-based sources of heralded single photons, that work by generating correlated photon pairs in photonic crystal fibre (PCF; also known as microstructured or holey fibre) [19] through the process of four-wave mixing (FWM) as a result of the  $\chi^{(3)}$  Kerr nonlinearity, have previously been demonstrated [20-22]. By pumping the fibre in the normal dispersion region close to the zero dispersion wavelength (ZDW) the generated photons are widely spaced in frequency on either side of the pump wavelength [20,23]. The resulting photon generated through FWM at a shorter wavelength than the pump is known as the signal photon and the corresponding generated photon at a longer wavelength is known as the idler photon. Being widely separated in wavelength means that the signal and idler photons can be easily

separated in fibre after generation. The controllable dispersion of photonic crystal fibre allows the idler and signal wavelengths to be selected via the phasematching condition for the nonlinear interaction [24]. Using narrowband filtering of the signal and idler photons, high purity single photon states have previously been demonstrated in fibre-based sources and interference effects between indistinguishable photons from two independent fibre-based sources have also been observed [25]. Fibre-based sources have already been used in the demonstration of quantum information processing applications [26].

A PCF with ZDW at 1087 nm was designed for use in this application. By pumping using picosecond pulses near 1064 nm the generated idler wavelength was at 1570 nm, near the wavelength of minimum attenuation of optical fibre and at a long enough wavelength to minimise the overlap with Raman shifted pump light. The corresponding signal wavelength was at around 800 nm, near the peak sensitivity of efficient silicon-based single photon detectors. As the photons are generated simultaneously, detection of the signal photon heralds the output of the corresponding idler photon.

## 2. Theory

The signal and idler photons necessary for the heralded photon source are generated in PCF by FWM. The PCF structure used was index guiding and endlessly single-mode [27] and is shown in Fig. 1.

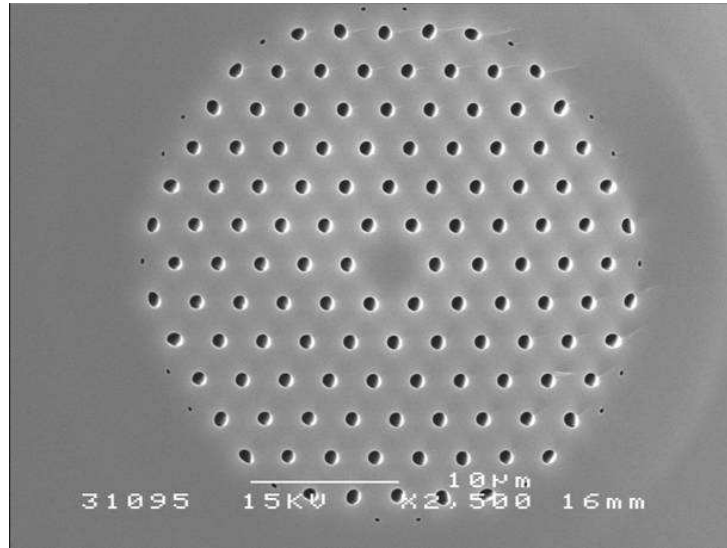


Fig. 1. SEM image of the PCF structure used. The core size is 5  $\mu\text{m}$  and the ratio of the air hole diameter to the pitch  $d/\Lambda$  is 0.33. The zero dispersion wavelength is 1087 nm.

The peak wavelengths for which the parametric amplification is efficient are determined by the energy and phasematching conditions:

$$\omega_s + \omega_i - 2\omega_p = 0 \quad (1)$$

$$k_s + k_i - 2k_p + 2\gamma P = 0 \quad (2)$$

where  $\omega_s$ ,  $\omega_i$ , and  $\omega_p$  are the frequencies of the signal, idler and pump photons respectively,  $k_s$ ,  $k_i$ , and  $k_p$  are the propagation constants for the signal, idler and pump,  $P$  is the peak pump power, and  $\gamma$  is the nonlinear coefficient of the fibre ( $\sim 7 \text{ km}^{-1} \text{ W}^{-1}$ ). Operating in the normal dispersion region close to the ZDW the contribution of the higher order terms of the dispersion become significant and the phasematched wavelengths are only weakly

dependent on the pump power. The calculated phasematching curve for the PCF used in this experiment is shown in Fig. 2.

The steep slope of the phasematching curve around the pump wavelength leads to gain over a range of several nanometers for the signal and idler, even for relatively narrowband pump pulses (<0.5 nm in this case). The calculated linewidth for a single frequency pump is less than 1 nm and is entirely swamped by the effect of the finite bandwidth pump. In order to achieve a narrowband source significant filtering of the generated FWM peaks was required, and this was implemented with narrowband fibre Bragg gratings. Assuming the FWM peaks have a  $\text{sech}^2$  profile and the same 4 ps pulse length as the pump pulse the required filter bandwidths are 0.15 nm at the signal wavelength and 0.6 nm at the idler wavelength respectively in order to produce time-bandwidth limited output photons. Fibre Bragg gratings with these bandwidths are commercially available, although for this experiment we used slightly broader gratings designed for a shorter pulse source.

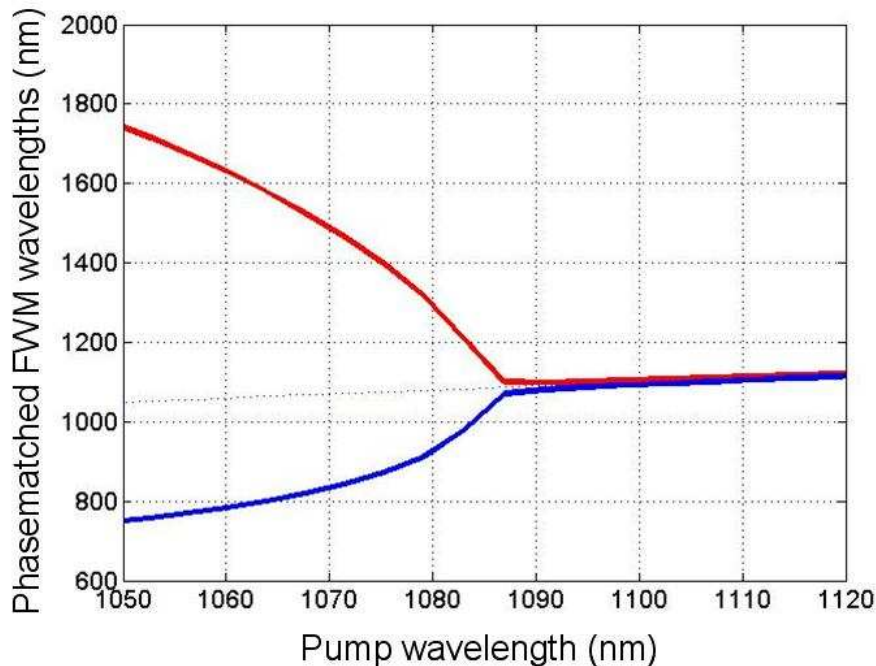


Fig. 2. Calculated phasematching curve for the PCF with a peak pump power of 12 W.

### 3. Experimental setup

The all-fibre source, the detectors used to characterise it, and the pump laser and launch optics are depicted in Fig. 3. The pump source used was a modelocked fibre laser (Fianium Ltd, *Femtomaster 1060-0.1*) with a central wavelength of 1063.2 nm. The pulse width was 4 ps at a repetition rate of 80 MHz, and the average power was adjustable up to a maximum of 100 mW. The pump light was passed through an optical isolator and a half wave plate ( $\lambda/2$ ), and then a prism in order to separate any photons present near the idler or signal wavelengths from the pump beam. The pump beam was then coupled into a 1.4 m section of the PCF using an anti-reflection coated aspheric singlet lens. Due to the input coupling efficiency of the PCF (around 60 %) and losses in the launch optics, a maximum power of 40 mW was available for nonlinear interaction in the PCF.

A fibre Bragg grating (FBG) with central wavelength 1064 nm spliced to the PCF provided 30 dB rejection of the pump light from the transmitted signal. A WDM system consisting of two fused fibre couplers then separated the generated idler and signal wavelengths into two separate fibres with low loss, whilst providing an additional 25 dB

rejection of the pump wavelength in both channels. Wavelength filtering in the idler arm of the device was achieved using a standard 1550 nm fibre circulator with a narrowband FBG spliced to the second port. The FBG had a central wavelength of 1569 nm and a bandwidth of 0.8 nm, providing near time-bandwidth limited filtering at the idler wavelength. Idler photons falling within this wavelength range were reflected back into the circulator and output from the third port. A spliced broadband FBG at 1064 nm provided additional rejection of pump light that was passing directly through the circulator from port 1 to port 3. The idler photons were then output into a 10 m section of single-mode fibre before being detected with an InGaAs based single-photon avalanche diode (ID Quantique, *ID200*). The time delay introduced into the idler arm by the extra section of fibre ensured that the idler photon arrived at the detector some time after the detection of the corresponding signal photon. The detection of a signal photon generated an electrical output that was used to trigger the detector in the idler arm. The InGaAs detector was operated at the minimum available electronic gate width of 2.5 ns. This corresponded to an actual time window of around 0.5 ns during which the detector was active and an idler photon could be detected.

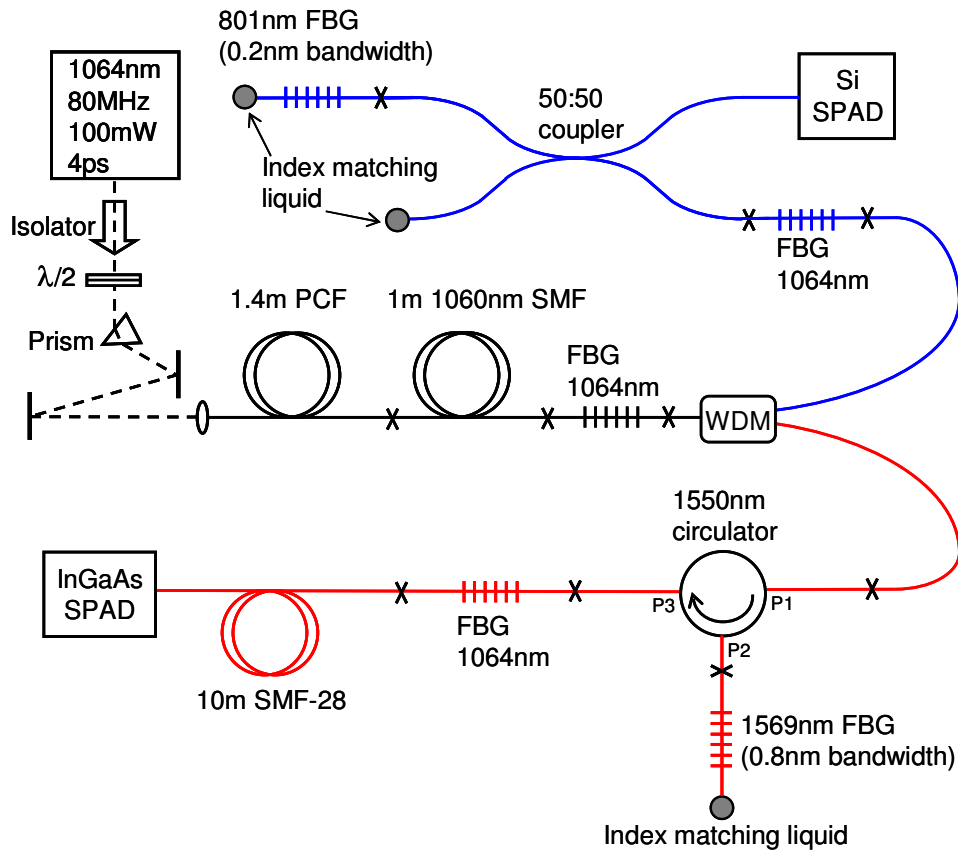


Fig. 3. Schematic diagram showing the all-fibre single photon source, the launch optics and detectors used.  $\lambda/2$  is a half wave plate and black crosses indicate splices. WDM consists of two spliced fused fibre wavelength division multiplexing components separating 803 nm, 1064 nm and 1570 nm light into different fibres, with a termination on the 1064 nm path.

In the signal arm filtering was achieved using a 50:50 fused fibre coupler with an FBG spliced to one of the two output ports. The FBG central wavelength of 801 nm and bandwidth of 0.2 nm were chosen in order to match the filtering of the signal photons to those in the idler arm. A spliced, broadband 1064 nm FBG was again used to provide additional rejection of the pump. The combination of FBGs, the WDM, and circulator and fused coupler ensured that the

calculated pump suppression was in excess of 100dB in both the signal and idler arms. Signal photons reflected back into the coupler and out through the second input port were detected using a Si based single-photon avalanche photodiode (Perkin Elmer, *SPCM-AQR-14*) and the electronic output from this detector was used to trigger the detector in the idler arm as described previously. The detection efficiency was 55 % at the signal wavelength.

The combination of a narrowband FBG with a circulator or fibre coupler provided the required narrowband filtering in both arms of the device [28]. The ends of the two narrowband FBGs were fixed to micrometer driven translation stages in order to apply strain. This allowed the central wavelengths of the two gratings to be tuned to match the signal and idler peak wavelengths for FWM gain. Triggering the InGaAs single-photon avalanche photodiode (SPAD) from the Si SPAD allowed the coincidence count rate between the two arms to be determined. The spare output fibre from the 50:50 coupler and the output ends of the narrowband FBGs were terminated in index matching liquid in order to avoid reflection of the pump light from the ends of the fibre.

#### 4. Results

After optimising the input coupling efficiency of the device for 1064 nm, a pump power of 65 mW (before the input end of the fibre) was applied to the device. The FBG central wavelengths were selected by first tuning the grating in the signal arm to achieve maximum singles count rate from the Si SPAD. The FBG in the idler arm was then tuned to approximately the matching wavelength, as determined by the energy matching condition given by Eq. 1. The Si SPAD was then used to trigger the detector in the idler arm to measure the coincidence count rate whilst the electronic delay in the InGaAs SPAD was varied. Once the time delay corresponding to coincident detection between the two arms was determined, the FBG in the idler arm could be tuned to maximise the coincidence count rate.

After optimising the central wavelengths of the narrowband FBGs the variation of the coincidence count rate as a function of the variable electronic delay in the measurement of the idler arm was measured. The large peak seen in Fig. 4 at around 10 ns delay corresponds to coincident detections of the signal and idler photons generated on the same pulse of the pump laser. The smaller peak at around 22 ns corresponds to uncorrelated detection events on a different pulse of the laser to that which produced the heralding signal photon. Statistically the main peak also contains the same number of accidental coincidences, so in all calculations the coincidence rate is the rate measured in the main peak with the rate measured in the subsidiary peak subtracted. The background coincidence count rate at delay times between these two peaks was around 30 counts per second. The detection efficiency of the InGaAs SPAD used in this measurement was 10 %, so the peak measured coincidence count rate of  $10^4$  counts per second corresponds to  $9.2 \times 10^4$  heralded single photons per second output from the device after subtraction of the 900 counts per second detected accidentals rate. The spectral brightness is  $1.15 \times 10^5$  photons per second per nanometer.

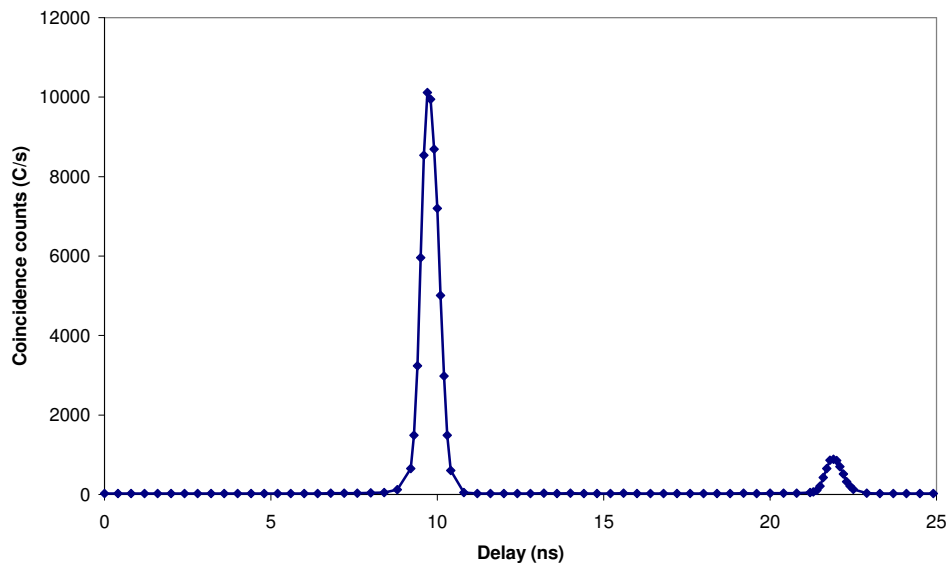


Fig. 4. Coincidence count rate between the two output arms of the device as a function of the variable electronic delay. This data was taken with a pump power of 65 mW incident on the PCF. The singles count rate in the signal arm was 180 kC/s at the main coincidence peak.

The ratio of the main coincidence counts peak to the smaller accidentals peak shown here is 10.4, again found after subtracting the accidentals rate from the measured peak coincidence count rate. Subsequently, measurements of the single photon count rate in the idler arm were made by triggering the InGaAs SPAD directly from the laser. This showed that the lumped efficiency in the signal arm (excluding the detector efficiency) was 4%. This was then used to calculate the generation rate of FWM mixing pair photons in this case as  $7.6 \times 10^6$  per second or 0.094 generated pairs per pulse. Assuming that there is no noise present in the count rates, the expected counts-to-accidentals ratio at this generation rate is 10.6. Comparing this value to the measured ratio of 10.4 shows that noise photons in the idler arm (such as leaked pump light and Raman shifted pump light) make up about 3% of the total counts in the accidentals peak. The dominant contribution to the accidentals peak is generated photon pairs and this places a fundamental limit on the amount of pump power that can be used in order to avoid multiple photon pairs being generated on a single pump pulse. For many applications a counts-to-accidentals ratio of 10 is considered to be an acceptable compromise between increasing the brightness of the single photon source and minimising the probability of multiphoton generation events in the PCF. For applications where there is less tolerance for errors the counts-to-accidentals ratio can be increased by reducing the pump power, although this also leads to a reduction in the brightness of the source. Fig. 5 shows the coincidence and accidentals peaks for the source operated at lower input power levels. In both cases the heralding fidelity remains above 50% and the counts to accidentals ratio improves with the decreased photon generation rate, as expected for a source with low noise.

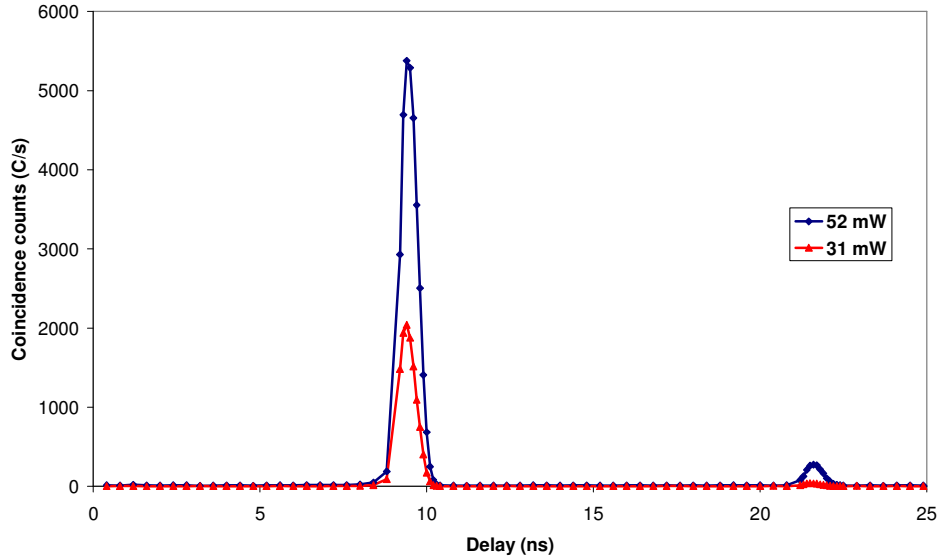


Fig. 5. Variation of the coincidence count rate with average input pump power. The measured counts-to-accidentals ratios were 18.6 and 46.5 for the high and low power cases respectively. At both pump powers the heralding fidelity was measured to be 51 %.

In addition to the counts-to-accidentals ratio, the heralding fidelity of the device is an important measure of the quality of the source. The heralding fidelity is the probability that a single photon is output, given that a heralding photon was detected in the signal arm, and can be calculated from the experimental data:

$$H = \frac{C - C_A}{N\eta} \quad (3)$$

where  $H$  is the heralding fidelity,  $C$  is the peak coincidence count rate,  $C_A$  is the accidentals count rate,  $N$  is the single photon count rate in the signal arm, and  $\eta$  is the InGaAs SPAD detection efficiency. The heralding fidelity of the device, calculated from the data shown in Fig. 4, was 52 %. Not only is this value close to the highest demonstrated for heralded single photon sources output into fibre [29] but this is achieved with narrowband filtering providing near time-bandwidth limited output single photons, and compares favourably with other recently demonstrated narrow bandwidth sources [28]. The high heralding fidelity was obtained by minimising the device loss between the point of generation and detection of the idler photons through careful choice of fibre components and low loss splicing.

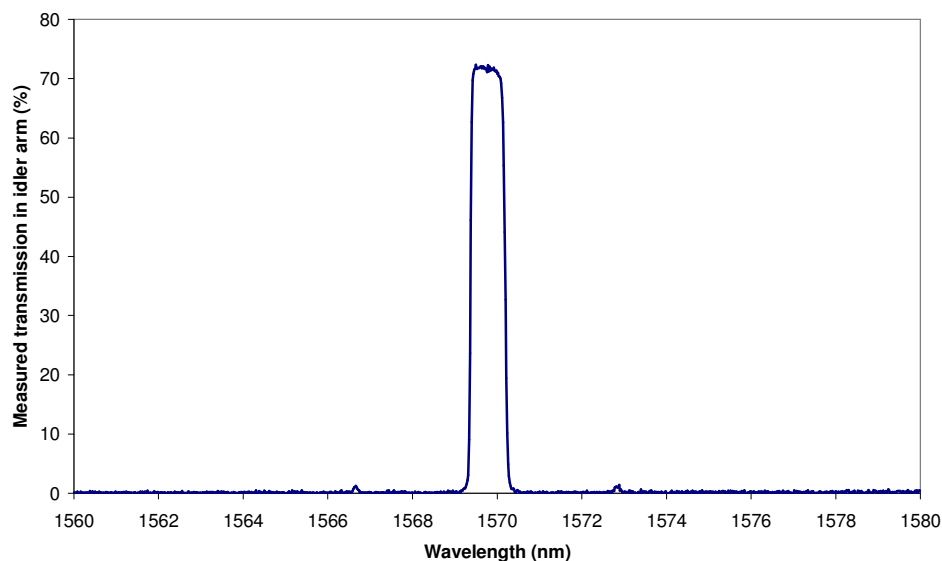


Fig. 6. Measured transmission of broadband light through the device from directly after the PCF to the InGaAs detector. The wavelength dependence of the transmission profile is due to the reflection from the narrowband fibre Bragg grating.

Figure 6 shows the measured passive transmission of the idler arm of the device, from the section of 1060 nm single-mode fibre (SMF) directly after the PCF, to the InGaAs SPAD. The splice loss between the PCF and SMF was measured separately and found to be  $-0.2\text{dB}$  at 1550 nm. These two measurements give the total transmission in the idler arm, from the PCF to the detector, as 68% ( $-1.63\text{dB}$ ). The main source of loss in the idler arm is the circulator, giving a combined insertion loss of  $0.9\text{dB}$  for the two paths. The discrepancy between the measured transmission and the lower than expected heralding fidelity may be due to the shape of the filtering introduced by the transmission profile of the narrowband FBGs. The wavelength of the generated single photons can also be determined indirectly from this transmission measurement as it corresponds to the central wavelength of the grating where peak transmission through the device occurs. The single photon wavelength was found to be near 1570 nm.

Currently the section of PCF used in the device is longer than the walk-off length of the three wavelengths involved in FWM. When combining two such single photon sources for interference in quantum information processing applications, this leads to a timing jitter that reduces the overlap between the interfering photons. Reducing the PCF to the calculated walk-off length of 30 cm should minimise this effect but will also reduce the coincidence count rate, although this could be compensated for by increasing the pump power. The brightness of the source could also be improved by replacing the 50:50 coupler with a fibre circulator. Currently the coupler introduces a loss of 6 dB to the signal arm so, in principle, the count rate could be quadrupled by this change. In practice the performance of circulators at 800nm is currently much worse than those operating around 1550nm and we might expect circulator losses of  $\sim 3\text{dB}$  and a doubling of the heralding rate. Finally this source employs no form of control over the output polarisation state of the heralded single photons. Polarisation maintaining PCF based on a similar fibre structure has already been produced [30] and low splicing losses to conventional fibre have been demonstrated. By replacing the PCF with a polarisation maintaining version and introducing polarisation control at the end of the device, the polarisation of the output single photon could be easily adjusted.

## 5. Conclusion

An all-fibre source of heralded single photons at 1570 nm was demonstrated. The operation of the source was based on generating a correlated pair of photons in a photonic crystal fibre through spontaneous four-wave mixing. The pair of photons were then separated into two single-mode fibres and suitably filtered. The detection of one photon of the pair then heralded the arrival of the other.

The source demonstrated both a high brightness of  $9.2 \times 10^4$  heralded photons per second, and a high heralding fidelity of 52 % with a counts-to-accidentals ratio of 10.4. Narrowband filtering in both the signal and idler arm meant that the output single photon state should be near time-bandwidth limited with a coherence length of 4ps. Being an all-fibre device, this source is easily produced, relatively low cost, compact, and the output is stable over time. Delivering the photon in single mode fibre also makes this device compatible with existing optical fibre systems. This bright narrowband heralded single photon source will find wide application in quantum information processing systems.

## Acknowledgments

The authors would like to thank Olivier Alibart for helpful discussions. This work was funded by the EPSRC (EP/F003560/1) and QIP IRC. W.J.W is a Royal Society University Research Fellow. J.G.R. is supported by a Wolfson Merit award.